High strength, superior fire retardancy and dimensional stability of cellulosic hybrids

Wen He [a,1,*], Rui Wang [a,1], Qunyan Pang [a], Ziliang Dai[a], Shuang Liang [a], Bairen Wei [a], Qiuling Ji [a], Wenxuan Li [a], Gangzheng Hu [a], Yue Jiao [a,*], Tripti Singh [b,c], Qiliang Fu [a,b,*]

[a] Co-Innovation Center of Efficient Processing and Utilization of Forest Resources, International Innovation Center for Forest Chemicals and Materials, College of Materials Science and Engineering, Nanjing Forestry University, Nanjing 210037, China

[b] Scion, 49 Sala Street, Private Bag 3020, Rotorua 3046, New Zealand

[c] National Centre for Timber Durability and Design Life, University of the Sunshine Coast, Sippy Downs, QLD 4556, Australia

[d] Fujian Joshine Bamboo Co., Ltd.

* Corresponding authors: hewen2011@njfu.edu.cn (W. He); Tel.: +86-138-0515-7249

jiaoyue@njfu.edu.cn (Y. Jiao); qiliang.fu@njfu.edu.cn (Q. Fu)

[1] These authors contributed equally to this work.

Table S1 Tensile strength.

Group	Tensile strength	Reference
Cellulose microfibril	1.6-3 GPa	[1]
Bamboo fiber	0.3-1.4 GPa	[2]
Nature bamboo	80-160 MPa	[3]

Table S2 The concentration of $CaCl_2$ solution and Na_2CO_3 solution.

Group	$CaCl_2$ concentration (mol/L)	Na_2CO_3 concentration (mol/L)
CMDB-0.1	0.1	0.1
CMDB-0.5	0.5	0.5
CMDB-0.9	0.9	0.9
CMDB-1.3	1.3	1.3

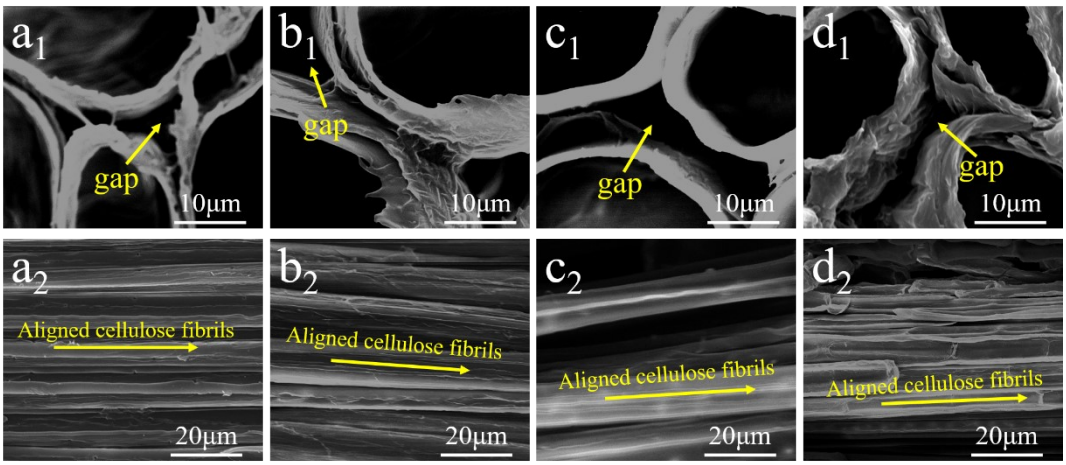

Fig. S1. Microstructure of (a) DB_2; (b) DB_4; (c) DB_6; (d) DB_8.

Table S3 The chemical compositions content of NB, DNB_2, DNB_4, DNB_6 and DNB_8.

Sample	Hemicellulose (%)	Cellulose (%)	Lignin (%)
NB	20.56	55.85	22.27
DB_2	16.98	70.08	11.32
DB_4	11.33	78.47	8.28
DB_6	10.63	85.48	1.02
DB_8	9.16	89.66	0.05

Note：Hemicellulose, cellulose and lignin are the main chemical components of bamboo. The rest fraction of the materials contains extractives and ash.

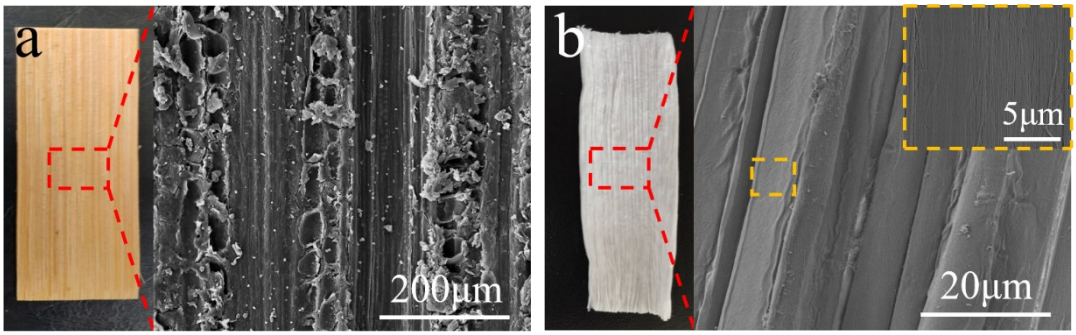

Fig. S2. Photographs and SEM images of the longitudinal section of (a) NB and (b) DB_6.

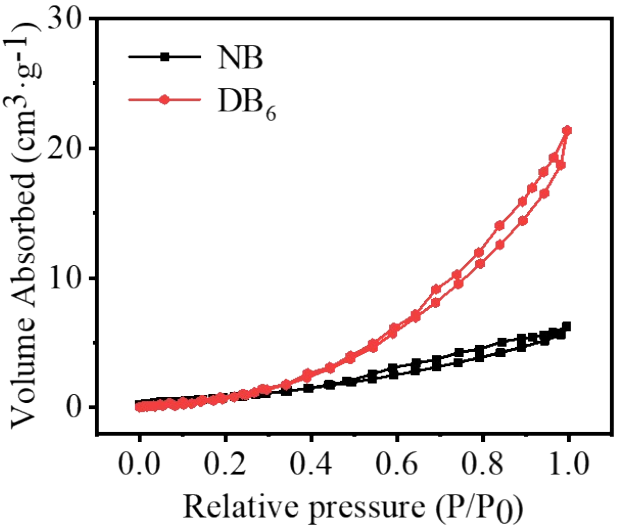

Fig. S3. Nitrogen adsorption-desorption isotherms of NB and DB_6.

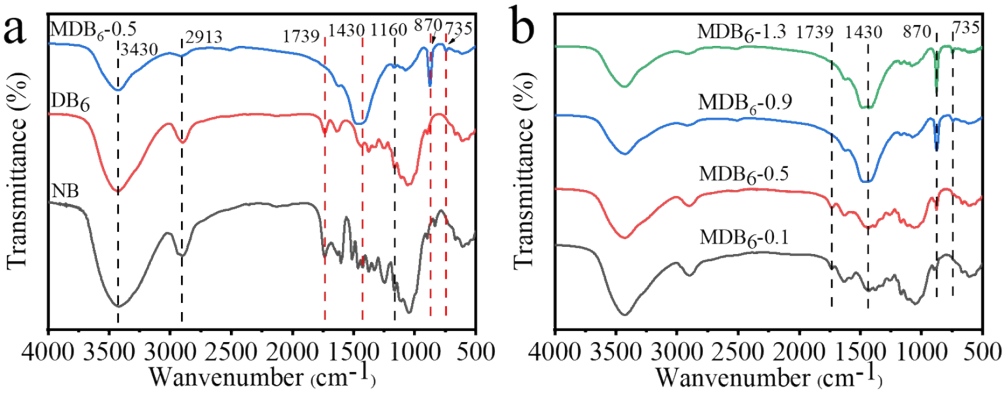

Fig. S4. FT-IR spectra of (a) NB, DB_6 and MDB_6-0.5 and (b) MDB_6 with different $CaCO_3$ concentration treatments.

Fig. S4a displays the FT-IR spectra of NB, DB_6 and MDB_6-0.5. The FT-IR spectrum of NB appears the distinct characteristic peaks of lignin, which are mainly located at 1631 cm^{-1} and 1505 cm^{-1}. However, these peaks disappeared from the FT-IR spectrum DB_6, which indicates the lignin was almost completely removed from the bamboo cells. The peaks at 2913 cm^{-1} and 1160 cm^{-1} are assigned to cellulose[4], the new peaks of 1430 cm^{-1} and 870 cm^{-1} appeared on the FT-IR spectrum of MDB_6-0.5, this ascribed to the non-vibrational stretching symmetry peak of C-O[5], and vibration peak of CO_3^{2-}, respectively. The intensity of characteristic peaks located at 1430 cm^{-1}, 870 cm^{-1} and 735 cm^{-1} significantly enhanced with the increase of mineralized concentration of $CaCO_3$ (Fig. S4b). The FT-IR results suggested that the $CaCO_3$ nanoparticles were successfully deposited on the DB_6.

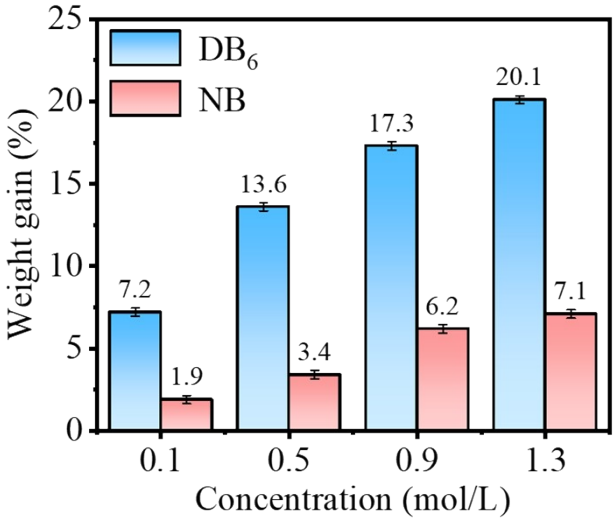

Fig. S5. The weight gain of NB and DB_6 with different $CaCO_3$ concentration treatment.

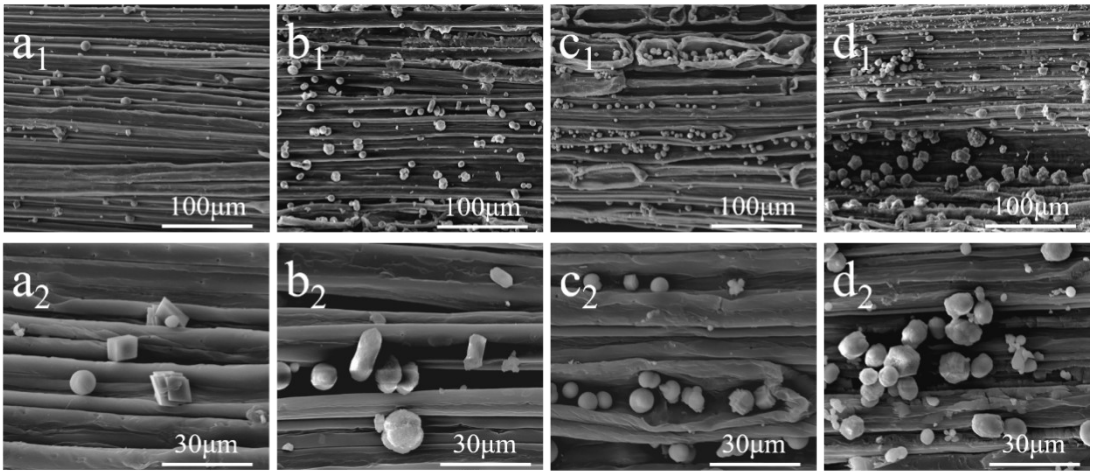

Fig. S6. SEM images of (a) MDB_6-0.1; (b) MDB_6-0.5; (c) MDB_6-0.9;(d) MDB_6-1.3.

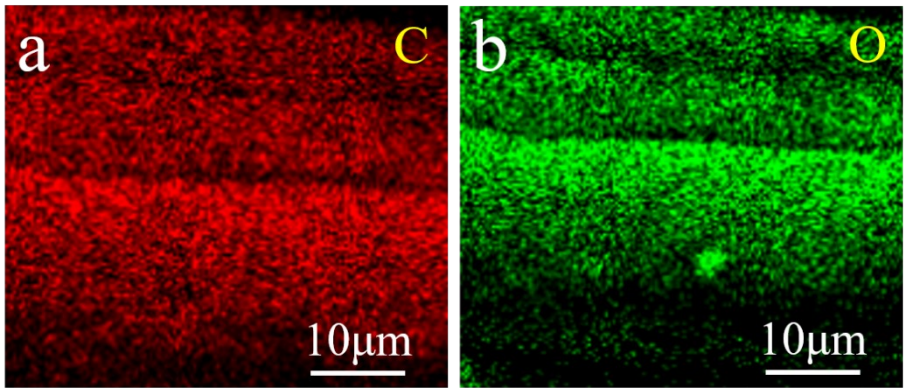

Fig. S7. (a) C element and (b) O element of MDB_6-0.5.

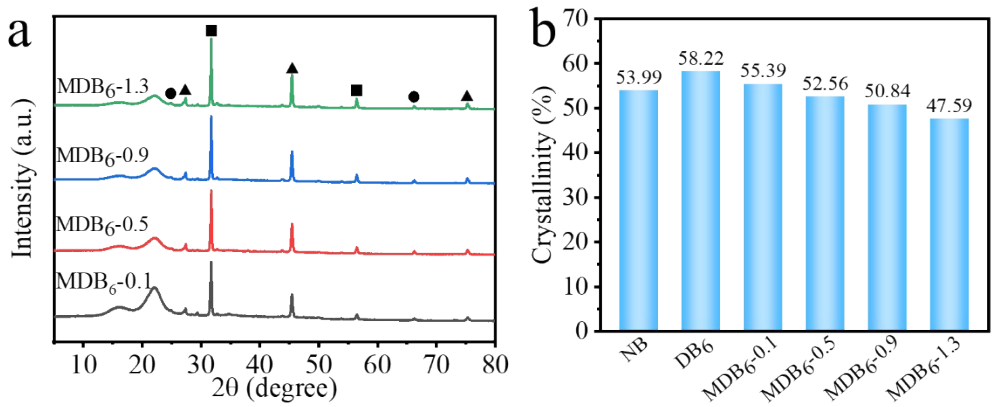

Fig. S8. (a) XRD curves of $MDNB_6$ with different $CaCO_3$ concentration treatments. (b) Crystallinity of NB, DNB_6 and $MDNB_6$ with different $CaCO_3$ concentration treatments.

The intensity of diffraction peaks of various $CaCO_3$ crystal significantly enhanced with the increase of concentration of Na_2CO_3 and $CaCl_2$ (Fig. S8a). The crystallinity degree of NB, DB_6 and all MDB_6 -0.5 specimens was calculated based on Segal method[6]. The crystallinity degree of the DB_6 specimen was about 58.22%, which is higher than that of NB (53.99%). However, the MDB_6-0.5 specimen showed a slightly lower crystallinity of 52.56% as the cellulose crystalline region was slightly hydrolyzed after the mineralization process. The crystallinity of MDB_6 significantly decreased due to the increase of concentration of Na_2CO_3 and $CaCl_2$ (Fig. S8b).

Table S4 Densities of all specimens.

Sample	Density(g/cm^3)
NB	0.67
DB_6	0.36
CDB	1.16
$CMDB_6$-0.1	1.18
$CMDB_6$-0.5	1.20
$CMDB_6$-0.9	1.21
$CMDB_6$-1.3	1.23

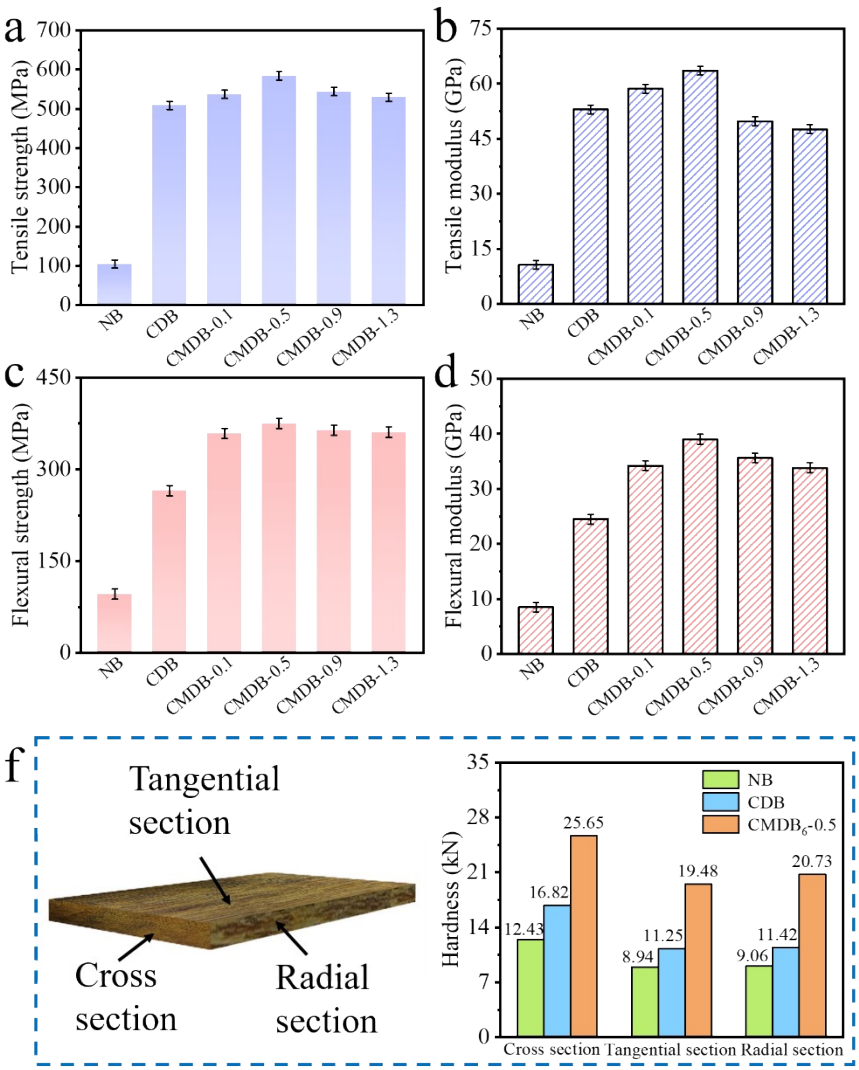

Fig. S9. (a) Tensile strength; (b) Tensile modulus; (c) Flexural strength; (d) Flexural modulus of all specimens. (f) Hardness of NB, CDB and $CMDB_6$-0.5.

The hardness of NB, CDB and CMDB-0.5 specimens was measured, as shown in Fig. S9f. The CMDB-0.5 specimen displayed the highest hardness value in cross-section (25.65 kN), tangential section (19.48 kN), and radial section (20.73 kN), respectively. Mineralization treatment resulted in the successive deposition of a $CaCO_3$ thin layer onto the cellulose microfibrils, significantly enhancing the hardness of CMDB specimens in three sections[7].

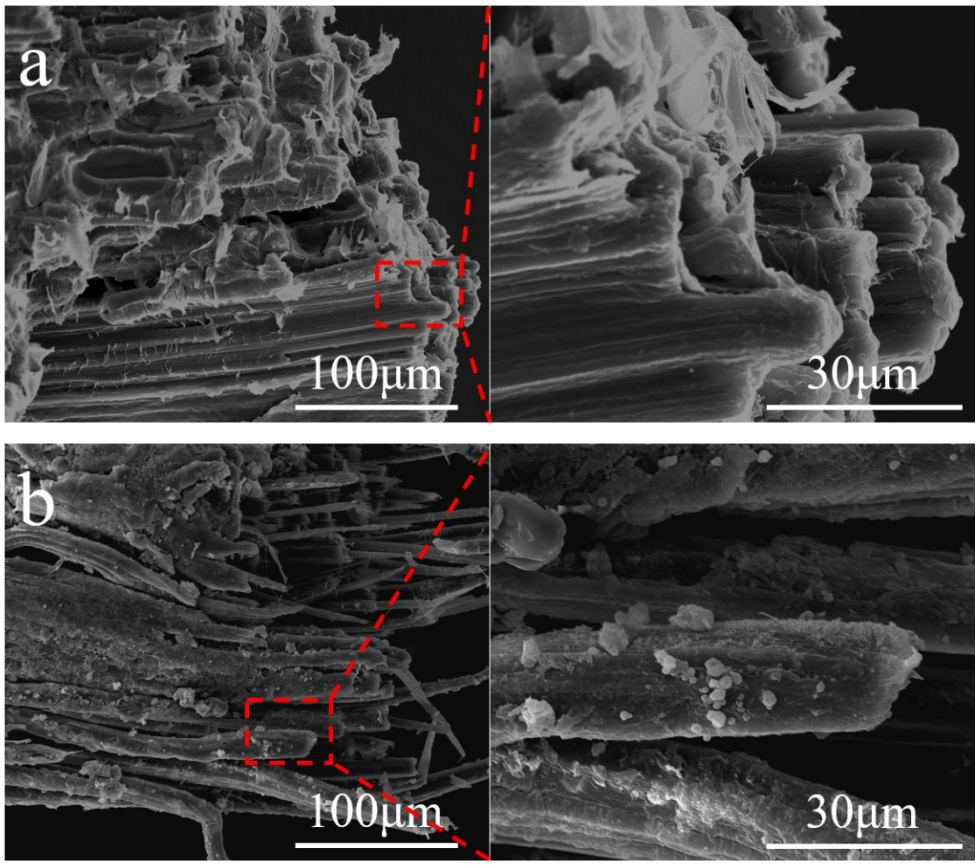

Fig. S10. SEM images of the tensile fracture surface of (a) CDB and (b) $CMDB_6$-0.5.

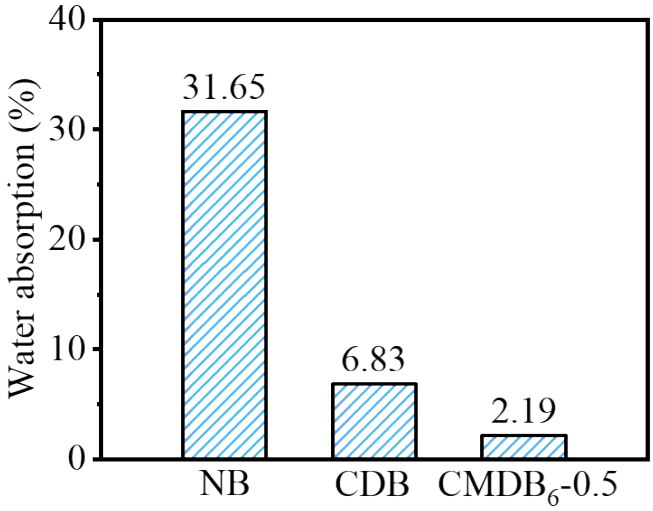

Fig. S11. Water absorption of NB, CDB and $CMDB_6$-0.5.

The water absorption of NB, CDB and CMDB-0.5 specimens is presented in Fig. S11. The NB specimen shows the highest value of 31.65%, and CMDB-0.5 has the lowest value of 2.19%. After hot-pressing, a large number of pore structures including the lumens of parenchyma cells and vascular bundle, as well as intercellular space are removed from CMDB-0.5, which dramatically reduces the capillary absorption of water. Meanwhile, the successive $CaCO_3$ and PF resin thin layer furtherly prevents the water from entering the bamboo fibers. Therefore, the water absorption of CMDB-0.5 was much lower than NB and CDB.

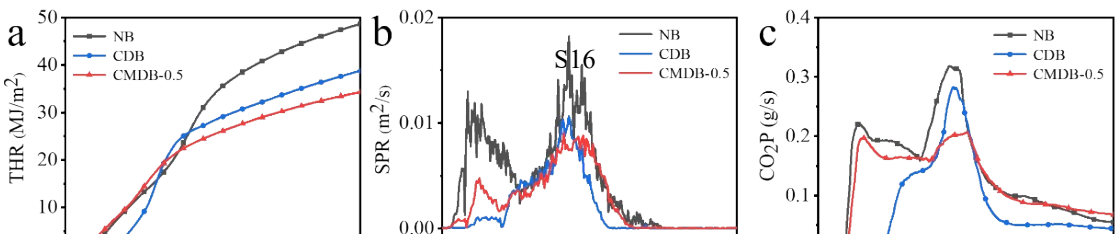

Fig. S12. (a) Total heat release; (b) smoke production rate; (c) CO_2 production rate of NB, CDB and CMDB-0.5.

The fire was ignited and spread rapidly for the NB with a total heat release (THR) was 76.9 MJ/m^2. The THR of CMDB-0.5 declined to 47.9 MJ/m^2 with a reduction of 37.7% compared to the NB specimen, and decreased by 17.9% compared to the CDB specimen (4 MJ/m^2) (Fig. S12a). The THR result shows that the mineralization of $CaCO_3$ could suppress the combustion intensity and ameliorate flame retardancy. This is in line with the result of the smoke production rate (Fig. S12b). The peak of smoke production rate for the CMDB-0.5 specimen showed the minimum values of 0.009 m^2/s with a reduction 50% and 18.2% compared with the NB and CDB specimens, respectively. Fig. S12c displayed the CO_2 production rate of the NB (0.32 g/s), CDB (0.28 g/s), and CMDB-0.5 (0.21 g/s). Compared with the NB and CDB specimens, the CO_2 production rate of the CMDB-0.5 specimen decreased by 34.4% and 25%, respectively.

Table S5 Comparison of the heat release rate and the total heat release of CMDB-0.5

with other materials.

Materials	HRR (Kw/m^2)	THR (MJ/m^2)	Reference
MB3	388.2	52.9	[8]
Coated bamboo	688.0	38	[9]
BBF1	443.2	62	[10]
Mineralized bamboo	260.5	45.3	[11]
MgAl-LB-6h	372.1	32.1	[12]
MTTO-b-ML	321.3	92.6	[13]
Ce-TNTs/bamboo fibre	548.6	36.4	[14]
BA-bamboo/epoxy	570.0	104.7	[15]
$H_2Ti_2O_5 \cdot H_2O$ TNTs/bamboo fiber	502.4	35.3	[16]
6%NCS-VE/BF	361.9	20.7	[17]
Bamboo fibre/ polypropylene	203.8	60.5	[18]
6%TNTs/bamboo fiber/HDPE	503.0	39.6	[19]
PP/wood powder/lignin	470	70.2	[20]
WPC/PATA$_1$/APP$_2$	310	80.3	[21]
EP-4.07-Wood	262.3	48.0	[22]
$CaCO_3$ beech	374.8	33.9	[23]
CMDB-0.5	**302.6**	**47.9**	**This work**

Note: MB3: mineralized bamboo (0.3mol/L $Ca(C_3H_5O_2)_2$ and Na_2CO_3). BBF1: bamboo fiber/PBS/microencapsulated ammonium polyphosphate composites. MgAl-LB-6h: bamboo with nano MgAl-layered double hydroxide coating. MTTO-b-ML: phosphorus-containing tung-oil-based polyol-coated melamine-modified bamboo. 6%NCS-VE/BF: chitosan-based bioflame retardant additive-vinyl ester/bamboo fiber. WPC/PATA1/APP2: wood-plastic composites/phytic acid-tyramine salt/ammonium polyphosphate. EP-4.07-Wood: wood with vanillin and benzene phosphorous oxydichloride coating.

Fig. S13. Photograph of the CMDB-0.5 of a large scale sample (16 cm in length, 2cm in width).

References

1. Z. H. Li, C. J. Chen, H. Xie, Y. Yao, X. Zhang, A. Brozena, J. G. Li, Y. Ding, X. P. Zhao, M. Hong, H. Y. Qiao, L. M. Smith, X. J. Pan, R. Briber, S. Q. Shi and L. B. Hu, *Nat. Sustain.*, 2022, **5**, 235-244.
2. J. K. Huang and W. B. Young, *Compos Part B-Eng*, 2019, **166**, 272-283.
3. H. Chen, H. T. Cheng, G. Wang, Z. X. Yu and S. Q. Shi, *J Wood Sci*, 2015, **61**, 552-561.
4. K. N. Guo, C. Zhang, L. H. Xu, S. C. Sun, J. L. Wen and T. Q. Yuan, *Bioresour. Technol.*, 2022, **354**, 9.
5. A. Stoica-Guzun, M. Stroescu, S. Jinga, I. Jipa, T. Dobre and L. Dobre, *Ultrason. Sonochem.*, 2012, **19**, 909-915.
6. H. Moura, L. M. A. Campos, V. L. da Silva, J. C. F. de Andrade, S. M. N. de Assumpcao, L. A. M. Pontes and L. S. de Carvalho, *Cellulose*, 2018, **25**, 5669-5685.
7. J. M. Xue, H. S. Ma, E. H. Song, F. Han, T. Li, M. Zhang, Y. F. Zhu, J. J. Liu and C. T. Wu, *Adv. Healthc. Mater.*, 2022, **11**, 11.
8. L. He, G. G. Bao, X. F. Zhang, X. F. Yue, Y. He and D. C. Qin, *Ind Crop Prod*, 2023, **202**, 117110.
9. C. H. Peng, J. H. Zhong, X. J. Ma, A. Huang, G. R. Chen, W. A. Luo, B. R. Zeng, C. H. Yuan, Y. T. Xu and L. Z. Dai, *Prog Org Coat*, 2022, **167**, 106830.
10. S. B. Nie, X. L. Liu, G. L. Dai, S. J. Yuan, F. Cai, B. X. Li and Y. Hu, *J. Appl. Polym. Sci.*, 2012, **125**, E485-E489.
11. L. He, G. G. Bao, X. B. Jin, R. Zhang and D. C. Qin, *Ind Crop Prod*, 2023, **197**, 116644.
12. X. L. Yao, C. G. Du, Y. T. Hua, J. J. Zhang, R. Peng, Q. L. Huang and H. Z. Liu, *J. Nanomater.*, 2019, **2019**, 9067510.
13. Z. W. Wang, S. L. Yang, Z. Liu, F. J. Ding, N. Ji and Y. Q. Wu, *Constr Build Mater*, 2023, **366**, 130240.
14. Z. L. Teng, C. L. Ye, C. M. Zheng, F. Chen, Y. Y. Li, S. L. Wen, J. Cai and P. Fei,

Polym Degrad Stabil, 2019, **168**, 108950.

15. W. W. Guo, E. N. Kalali, X. Wang, W. Y. Xing, P. Zhang, L. Song and Y. Hu, *Ind Crop Prod*, 2019, **138**, 111478.
16. C. M. Zheng, S. L. Wen, Z. L. Teng, C. L. Ye, Q. L. Chen, Y. H. Zhuang, G. G. Zhang, J. Cai and P. Fei, *Cellulose*, 2019, **26**, 2729-2741.
17. M. N. Prabhakar, K. V. Chalapathi, A. U. R. Shah and J. Song, *Cellulose*, 2021, **28**, 11625-11643.
18. X. B. Jin, E. L. Xiang, R. Zhang, D. C. Qin, Y. He, M. L. Jiang and Z. H. Jiang, *J Mater Res Technol*, 2022, **17**, 3138-3149.
19. P. Fei, X. Chen, H. G. Xiong, D. Zia ud, L. Chen and J. Cai, *Compos. Pt. A-Appl. Sci. Manuf.*, 2016, **90**, 225-233.
20. L. N. Liu, M. B. Qian, P. A. Song, G. B. Huang, Y. M. Yu and S. Y. Fu, *Acs Sustain Chem Eng*, 2016, **4**, 2422-2431.
21. Y. M. Leng, X. Zhao, T. Fu, X. L. Wang and Y. Z. Wang, *Acs Sustain Chem Eng*, 2022, **10**, 5055-5066.
22. M. L. Li, X. H. Hao, M. L. Hu, Y. S. Huang, C. Tang, Y. Y. Chen and L. P. Li, *Prog Org Coat*, 2022, **172**, 107161.
23. A. Pondelak, A. S. Skapin, N. Knez, F. Knez and T. Pazlar, *Green Chem.*, 2021, **23**, 1130-1135.